CHAPTER 8

AM J PHYSIOL RENAL PHYSIOL 2013; 305:F901-1

Renal ischemia/reperfusion induces a dysbalance of angiopoietins, accompanied by proliferation of pericytes and fibrosis

Meriem **KHAIROUN***, Pieter **VAN DER POL***,
Dorottya K. **DE VRIES**, Ellen **LIEVERS**, Nicole **SCHLAGWEIN**,
Hetty C. **DE BOER**, Ingeborg M. **BAJEMA**, Joris I. **ROTMANS**,
Anton Jan **VAN ZONNEVELD**, Ton J. **RABELINK**,
Cees **VAN KOOTEN**, Marlies E.J. **REINDERS**

*authors contributed equally

ABSTRACT

Introduction: Endothelial cells (ECs) are highly susceptible to hypoxia and easily affected upon ischemia/reperfusion (I/R) during renal transplantation. Pericytes and angiopoeitins play important role in modulating EC function. In the present study, we investigate the effect of renal I/R on dynamics of angiopoietin expression and its association with pericytes and fibrosis development.
Methods: Male Lewis rats were subjected to unilateral renal ischemia for 45 minutes followed by removal of the contralateral kidney. Rats were sacrificed at different time points after reperfusion. Endothelial integrity (RECA-1), pericytes (PDGFRβ), Angiopoietin-2 (Ang-2)/Angiopoietin-1 (Ang-1) expression and interstitial collagen deposition (Sirius Red and α-SMA) were assessed using immunohistochemistry and RT-PCR.
Results: Our study shows an increase in protein expression of Ang-2 starting at 5 hours and remaining elevated up to 72 hours, with consequently higher Ang-2/Ang-1 ratio after renal I/R ($p<0.05$ at 48 hours). This was accompanied by an increase in protein expression of the pericytic marker PDGFRβ and a loss of ECs (both at 72 hours after I/R, $p<0.05$). Nine weeks after I/R, when renal function was restored, we observed normalization of the Ang-2/Ang-1 ratio and PDGFRβ expression and increase in cortical ECs, which was accompanied by fibrosis.
Conclusions: Renal I/R induces a dysbalance of Ang-2/Ang-1 accompanied by proliferation of pericytes, EC loss and development of fibrosis. The Ang-2/Ang-1 balance was reversed to baseline at 9 weeks after renal I/R, which coincided with restoration of cortical ECs and pericytes. Our findings suggest that angiopoietins and pericytes play an important role in renal microvascular remodeling and development of fibrosis.

INTRODUCTION

Renal I/R is an inevitable consequence of renal transplantation causing significant graft injury (5;16;29). Renal I/R impairs the integrity of ECs and leads to loss of peritubular capillaries (6;9;17;19;25;32;36). Loss of integrity and function of the endothelial monolayer lead to renal hypoxia, which is suggested to be a major initiator of profibrotic changes and interstitial scar formation in the kidney (2;24). These microvascular changes and renal scarring eventually lead to a deteriorating of renal function and graft loss (26).
Pericytes play a critical role in the stabilization and proliferation of peritubular capillaries via interaction with ECs (1;20;30). This process is mediated by several angioregulatory factors, including Ang-1, produced by pericytes and Ang-

2 produced by activated ECs (7;30;35). Angiopoietins are a group of vascular regulatory molecules that bind to the receptor tyrosine kinase Tie-2, which is predominantly expressed by vascular ECs. Ang-1 is a strong vascular protective agonist of the Tie-2 receptor responsible for suppressing vascular leakage, maintaining EC survival and inhibiting vascular inflammation. Ang-2 acts as an antagonist of Ang-1 and in a dose dependent manner promotes destabilization, vessel leakage and inflammation. By promoting pericyte dropout, Ang-2 will lead to loosening contacts between ECs and perivascular cells, with subsequent vessel destabilization and abnormal microvascular remodeling (7;14;15;35). Recent studies have shown that pericytes detach from the endothelium and migrate to the interstitium to become activated and differentiate into myofibroblasts contributing to renal fibrosis (10;12). Interestingly, treatment with cartilage oligomeric matrix protein (COMP)-Ang-1 in a mice model of renal I/R injury resulted in protection against peritubular capillary damage and decrease in inflammatory cells and renal interstitial fibrosis (19).

However, dynamics and the time course of angiopoietin expression, its relation with EC and pericyte expression and development of fibrosis in the repair phase after renal I/R injury are unknown. Using an established rat model of renal I/R injury, we assessed the impact of I/R on Ang-2/Ang-1 balance and its effect on microvascular remodeling, pericytes and the formation of fibrosis up to 9 weeks after renal I/R injury. We hypothesize that I/R injury leads to activation of ECs with consequent elevation of Ang-2 levels, which may lead to proliferation of pericytes and loss of ECs, but may also induce fibrosis in the long term.

METHODS

Rat model of renal I/R injury

Renal I/R injury was induced as previously described (34). The Animal Care and Use Committee of the Leiden University Medical Center approved all experiments. Eight-week-old male Lewis rats (200–250 g) purchased from Harlan (Horst, The Netherlands) were housed in standard laboratory cages and allowed free access to food and water throughout the experiments. Unilateral ischemia was induced by clamping of the left renal pedicle for 45 min using a bulldog clamp (Fine Science Tools, Heidelberg, Germany). During clamping the contralateral kidney was removed. Sham-treated rats had identical surgical procedures except for clamping of the left kidney. Tail blood samples were taken before and at indicated time points after reperfusion and were kept on ice. Rats were sacrificed at 2, 5, 24, 48 or 72 hours (hr) and 1, 6 and 9 weeks (wk) after reperfusion and kidneys were harvested for histological examination and immunohistochemical staining.

Renal function was assessed by measuring creatinine and urea (BUN) in serum samples using standard auto analyzer methods by our hospital research services.

Immunohistochemistry and immunofluorescent staining

Rat kidney sections (4 μm) of snap-frozen kidneys were air dried and acetone fixed. Slides were incubated overnight with goat polyclonal IgG against Ang-1 (N18) or Ang-2 (F18; both Santa Cruz Biotechnology), mouse monoclonal IgG against endothelial cells (RECA-1; Hycult Biotechnology, Uden Netherlands and CD31; Abcam, Cambridge, England), myofibroblasts (α-SMA, Progen, Heidelberg, Germany), inflammatory cells (OX42+ for monocytes, dendritic cells and granulocytes, and CD45 (BD Pharminghen, Breda Netherlands) for leukocytes) or rabbit polyclonal IgG against pericytes (PDGFRβ; Abcam, Cambridge, England). Antibody binding was detected with horseradish peroxidase (HRP)-labeled rabbit anti-goat IgG (DAKO, Glostrum, Germany), goat anti-mouse IgG (Jackson, Suffolk, England) or goat anti-rabbit IgG (DAKO), respectively. After washing, sections were incubated with tyramide-fluorescein isothiocyanate in tyramide buffer (NENTM Life Science Products, Boston, MA, USA), washed and incubated with HRP-labeled rabbit anti-fluorescein isothiocyanate (DAKO, Glostrum, Germany) and developed with 3,3'-Diaminobenzidine (DAB) (Sigma, St Louis, MO, USA). Sections were counterstained with haematoxylin (Merck, Darmstadt, Germany) and mounted with imsol (Klinipath, Duiven, the Netherlands). Quantification of immunohistochemistry was performed in a blinded manner by assessing consecutive high power fields (magnification, ×100) on each section from the cortex, outer and inner medulla. Using Image J software, the percentage of positivity per specific region of the kidney was determined, with exception of Ang-1 and Ang-2, which was only analyzed for the cortex. Glomeruli were excluded from all analyses of the cortex. Since the Ang-2/Ang-1 ratio, rather than the absolute expression of either angiopoietin is generally used to determine the functional status of the microvasculature (26), this ratio was calculated using the Ang-2 and Ang-1 quantification. Immunofluorescent double stainings were performed for ki-67 (cell proliferation marker) using polyclonal rabbit IgG (Abcam, Cambridge, England) and RECA-1 and Ang-2/RECA-1. Due to technical reasons double stainings with Ang-1/ PDGFRβ and RECA-1/ PDGFRβ could not be performed, therefore the pericyte marker NG2 (rabbit polyclonal IgG; BD Pharmingen, Breda, Netherlands) was used for these double stainings. Antibody binding was visualized using Alexa™ 488-labeled goat anti-rabbit IgG, Alexa™ 568-labeled goat anti-mouse IgG (both Life science) and donkey anti-goat IgG (Jackson, Suffolk, England). Nuclei were stained using Hoechst (Molecular Probes, Leiden, the Netherlands). Micrographs were made using a fluorescence microscope (Leica, DMI6000, Rijswijk, the Netherlands).

Histologic evaluation

Renal fibrosis was evaluated histologically by Sirius Red staining as described previously (27) on 4 µm paraffin slides of renal rat tissue. From each part of the kidney (cortex, outer and inner medulla) five random images were obtained. Image analyses was performed using Image J software. The amount of collagen deposition was measured and expressed as percentage of positivity per region of the kidney. In addition, all tissue specimens were scored for severity of fibrosis on a semi-quantitative scale (0-3) in a blinded manner by an experienced pathologist.

RNA isolation and Real-Time PCR

RT-PCR was performed as described previously (34). Total RNA was extracted from snap frozen cross-section kidney slices using the RNeasy Mini isolation Kit according to the manufacturer's instructions (QIAGEN, Hilden, Germany). cDNA was synthesized from 1 µg total RNA, using an oligo dT primer, RNase-OUT, M-MLV reverse transcriptase, 0.1 M-DTT and buffers in a volume of 20 µL (all purchased from Invitrogen, Breda, The Netherlands). Quantitative real-time PCR was performed in duplicate by using iQ SYBR Green Supermix on iCycler Real-Time Detection System (BioRad). The amplification reaction volume was 20 µL, consisting of 10 µL iQ SYBR Green PCR mastermix, 1 µL primers, 1 µL cDNA, and 8 µL water. Data were analyzed using Gene Expression Analysis for iCycler Real-Time PCR Detection System (Biorad). Expression of each gene was normalized against mRNA expression of the housekeeping gene Rsp-15. RT PCRs were performed in duplicate. The primer sequences are shown in table 1.

Table 1. Primer sequences used for quantitative real-time PCR

Gene	Forward primer 5'->'3	Reverse primer 5'->'3	Supplier
RSP-15	CGTCACCCGTAATCCACC	CAGCTTCGCGTATGCCAC	Biolegio
ANG-1	TCTCTTCCCAGAAACTTCA	TTTGATTTAGTACCTGGGTCTC	Biolegio
ANG-2	TGCATCTGCAAGTGTTCCC	GCCTTGAGCGAGTAACCG	Biolegio
TIE-2	GTCCTATGGTGTATTGCTCTG	TCTCTCATAAGGCTTCTCCC	Biolegio

Statistical analyses

Data are reported as mean ± standard error of the mean (SEM). Statistical comparisons were performed using one-way ANOVA or Mann–Whitney test with GraphPad Prism software (GraphPad Software Inc., San Diego, CA, U.S.A.). A value of $p < 0.05$ was considered statistically significant.

RESULTS

Renal I/R induces transient deterioration of renal function, influx of inflammatory cells and interstitial fibrosis

In the current study we used a rat model of renal I/R resulting in extensive renal dysfunction, as shown by increased serum creatinine and BUN levels, but characterized by normalized renal function after 1 week following I/R ($p<0.05$, compared to 72 hr) (Fig. 1A, B). Renal dysfunction was accompanied by significant

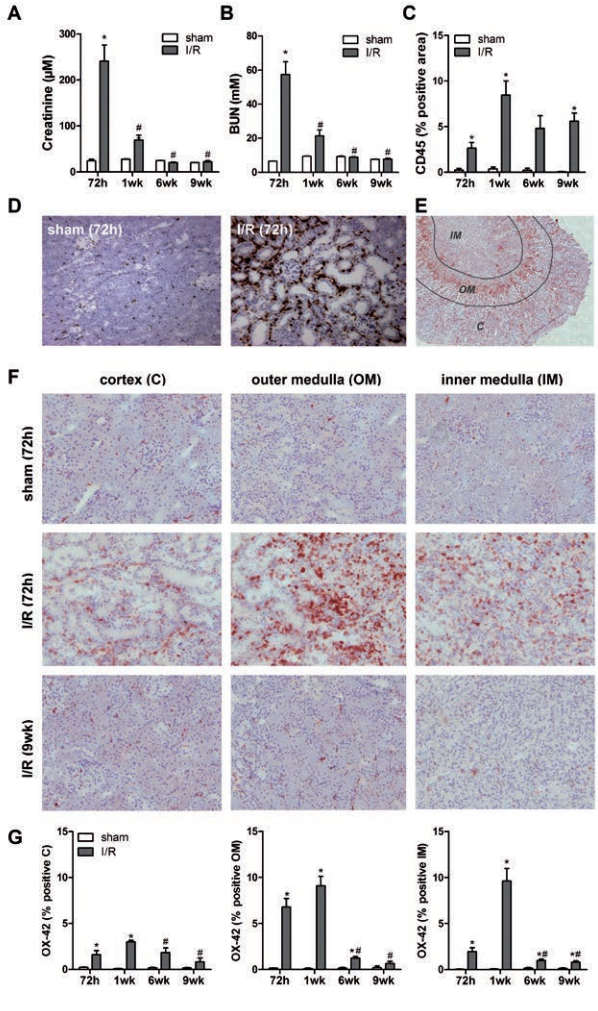

Figure 1. Renal I/R induces deterioration of renal function and influx of inflammatory cells. Serum creatinine levels (A) and BUN (B) were measured at consecutive time points after reperfusion. CD45+ leukocyte infiltrate was quantified using digital image analysis (C). Representative photomicrographs of kidney sections stained with CD45 (D) from a sham-operated rat and a rat subjected to I/R and sacrificed at 72 hr after reperfusion. An overview of the division of the different regions (cortex, outer medulla and inner medulla) in a kidney section stained with OX42 (E). Representative photomicrographs of kidney sections stained with OX42+ from a sham-operated rat and rats subjected to I/R and sacrificed at 72 hr or 9 weeks after reperfusion (F). OX42+ infiltrate of sham-operated rats and rats subjected to I/R was quantified in the different areas using digital image analysis (G) and demonstrated as % of the depicted area. Data are shown as mean ± SEM (n= 5 rats per group). *P<0.05 compared to corresponding sham controls. #P<0.05 compared to 72 hr or 1 wk rats. Original magnification of D, E and F, x200. C=cortex; OM=outer medulla; IM=inner medulla.

infiltration of OX42+ inflammatory cells in the cortex, outer and inner medulla at 72 hr ($p<0.05$), which peaked at 1 week compared to sham-operated rats (Fig. 1E, F, G). A decrease in OX42+ inflammatory cells was observed at 6 and 9 weeks in the different parts of the kidney compared to 1 week following I/R ($p<0.05$). In the outer and inner medulla, the influx of OX42+ cells remained significantly increased up to 6 and 9 weeks ($p<0.05$), respectively, after renal I/R injury

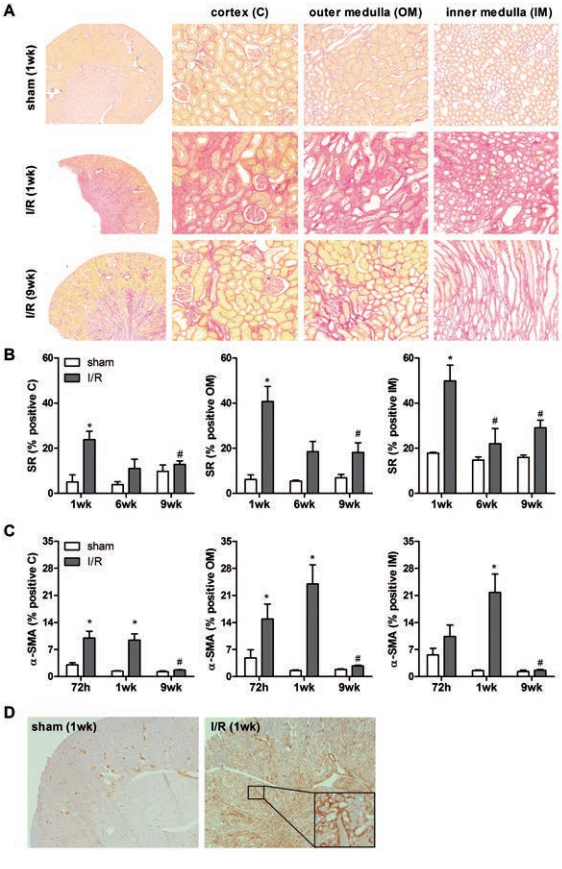

Figure 2. Renal I/R induces interstitial fibrosis. Representative photomicrographs of Sirius Red stained kidney sections (A) of the cortex, outer medulla and inner medulla obtained from a sham-operated rat (sacrificed at 1 week), and rats subjected to I/R and sacrificed at 1 or 9 weeks after reperfusion as indicated. Quantitative analysis of Sirius Red staining (B) and α-SMA staining (C) at different time points after reperfusion in sham-operated rats and rats subjected to I/R in the different regions as indicated. Quantification was performed by digital image analysis and is demonstrated as % of the depicted area. Data are shown as mean ± SEM (n= 5 rats per group). *P<0.05 compared to corresponding sham controls. #P<0.05 compared to 72 hr or 1 wk rats. Original magnification of A, x200. C=cortex; OM=outer medulla; IM=inner medulla.

compared with sham-operated rats (Fig. 1G). Consistently, CD45 expression in the cortex showed a similar pattern as OX42+ staining (Fig. 1C, D).

One week after reperfusion, significant diffuse interstitial collagen deposition was observed in the cortex, outer and inner medulla compared to sham-operated rats ($p<0.05$) (Fig. 2A, B). After 9 weeks collagen deposition was significantly decreased in different regions of the kidney compared to 1 week following renal I/R injury ($p<0.05$), although kidneys were still characterized by focal areas of intense Sirius Red staining. The semi-quantitative analyses showed that fibrosis scores at 9 weeks were not statistically different from 1 week after I/R (data not

shown), which is probably due to the focal areas of fibrosis. Consistently, the α-SMA immunohistochemical staining revealed a significant increase of fibrosis in cortex and outer medulla at 72 hr ($p<0.05$) and at all parts of the kidney at 1 week ($p<0.05$) following I/R injury compared with sham-operated rats (Fig. 2C, D). At 9 weeks, α-SMA staining was significantly decreased in the cortex, outer and inner medulla compared with 1 week after I/R injury (Fig. 2C).

Restoration of peritubular capillaries in the cortex after renal I/R

Since endothelial damage is an important hallmark of I/R injury, we assessed peritubular capillaries over time by staining for RECA-1. A significant reduction in RECA-1 expression was observed at 72 hr post I/R ($p<0.05$) in the cortex and

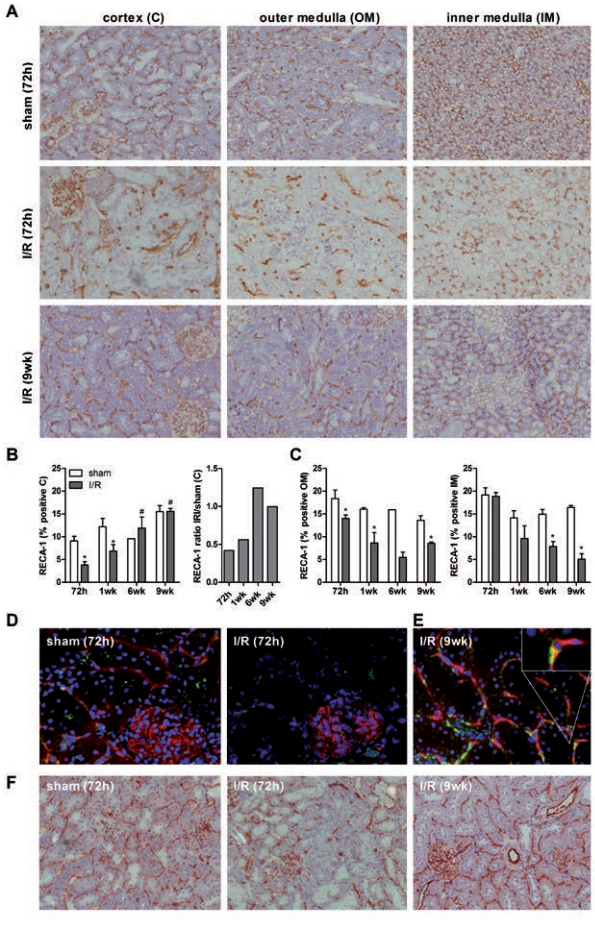

Figure 3. Restoration of I/R-induced peritubular capillary loss in the cortex late after reperfusion.
Representative images of kidney sections of the cortex, outer medulla and inner medulla stained for RECA-1 (A) obtained from a sham-operated rat and rats subjected to I/R and sacrificed at 72 hr and 9 weeks after reperfusion. RECA-1 was quantified using digital image analysis as indicated (B). Immunofluorescent double staining for RECA-1 (red) and Ki-67 (green) of representative kidney sections of a sham-operated rat and rats sacrificed at 72 hr (C) or 9 weeks (D) after reperfusion. Insert is showing double positivity of RECA-1 and Ki-67 staining in yellow in kidney sections at 9 weeks after reperfusion. Representative images of kidney sections of the cortex stained for CD31 (E) obtained from a sham-operated rat and rats subjected to I/R and sacrificed at 72 hr or 9 weeks after reperfusion. Data are shown as mean ± SEM (n= 5 rats in grouper group). *P<0.05 compared to corresponding sham controls. #P<0.05 compared to 72hr. Original magnification of A, C and E, x200; insert at 9 weeks, x400.

outer medulla and at 1 week in the inner medulla ($p<0.05$) compared with sham-operated rats (Fig. 3A, B). Interestingly, we found a significant increase of RECA-1 staining at 6 and 9 weeks in the cortex ($p<0.05$) following I/R compared to rats that were sacrificed at 72 hr (Fig. 3B). RECA-1 staining colocalized with the proliferation marker Ki-67, suggesting EC proliferation in peritubular capillaries within the renal cortex at 9 weeks after I/R (Fig. 3C). No proliferation of ECs was found in the glomeruli following renal I/R. In the outer and inner medulla a different pattern was found. Here, a significant reduction in RECA-1 expression was observed at 72 hr post I/R in the outer medulla ($p<0.05$) and at 1 week in the inner medulla ($p<0.05$) compared with sham-operated rats (Fig. 3B). In contrast to the cortex, RECA-1 staining in these areas showed a further decrease up to 9 weeks after ischemic injury ($p<0.05$) (Fig. 3B). CD31 staining demonstrated a pattern comparable to the RECA-staining (Fig. 3E).

Renal I/R induces a dysbalance in Ang-2/Ang-1 ratio at early time points and return to baseline after 6 weeks

In control kidneys of sham-operated rats, Ang-1 staining was observed in the glomeruli and in a capillary like pattern between the tubuli (Fig. 4A). Double staining of Ang-1 and the pericyte marker NG2 revealed colocalization, suggesting that Ang-1 is expressed by pericytes (Fig. 4C). Starting at 24 hr after renal I/R, a significant decrease in Ang-1 expression was observed (data not shown), reaching a maximal decrease at 72 hr ($p< 0.05$) (Fig. 4A, F). Ang-1 expression increased significantly at 9 weeks after renal I/R compared to 72 hr ($p<0.05$) (Fig. 4A, F). Additionally, RT-PCR analyses revealed a decrease in Ang-1 mRNA levels which reached significance at 1 week compared the sham-operated rats ($p<0.05$; Fig. 4I). In control rats, low levels of Ang-2 protein were observed in glomeruli, interstitial vessels and on brushborders of tubuli (Fig. 4B, G). Due to the apical and brush border expression on tubuli of Ang-2 in the medulla, it was technically not possible to distinguish between interstitial and tubular presence of Ang-2 (Fig. 4E). Therefore quantification of angiopoietins was only performed in the cortex. Additional double staining of Ang-2 and RECA-1 confirmed the expression of Ang-2 by ECs (Fig. 4D). Compared to sham-operated rats, Ang-2 expression increased at 5 hr (data not shown) and remained elevated up to 72 hr ($p< 0.05$) after I/R (Fig. 4G). Consequently higher Ang-2/Ang-1 ratios were observed after 48 hr and 72 hr ($p<0.05$) (Fig 4H). After 1 week, Ang-2 levels and Ang-2/Ang-1 ratio started to decrease, reaching significance at 6 and 9 weeks compared to 72 hr after renal I/R (Fig. 4B, G and H). Ang-2 mRNA levels did not confirm the observed changes at protein levels (Fig. 4J). Tie-2 mRNA expression showed a significant decrease at 1 week compared with sham-operated group and reversal to baseline levels at 9 weeks after I/R (Fig. 4K).

Renal I/R leads to proliferation of pericytes

Immunohistochemical staining revealed the presence of PDGFRβ positive cells in the mesangium, Bowman's capsule, large vessels and peritubular capillaries (Fig. 5A). A significant increase of pericytes was observed at 48 hr upon I/R in all parts of the kidney compared with sham-operated rats, which persisted up

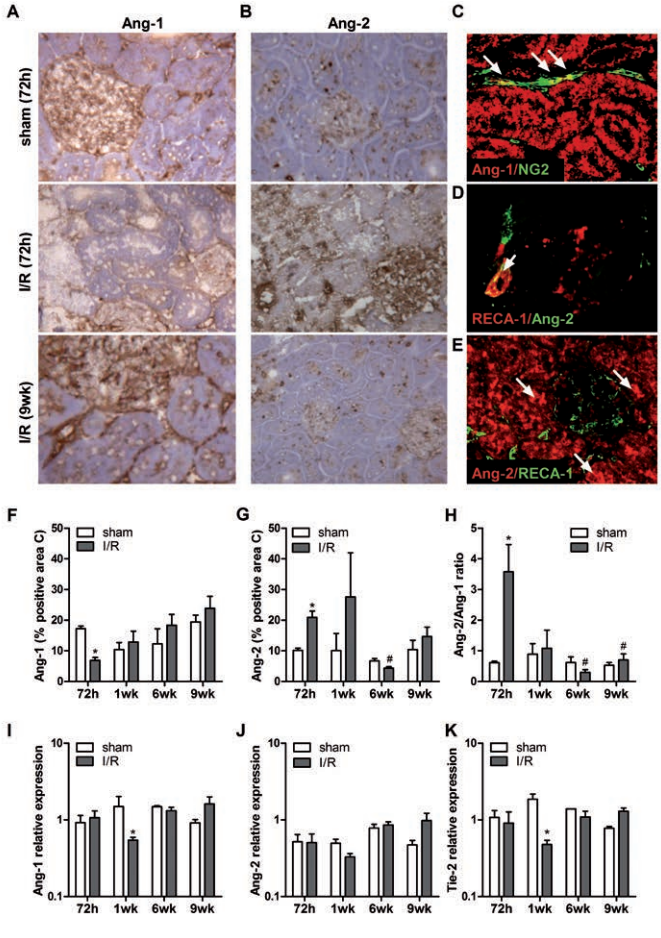

Figure 4. Renal I/R induces a dysbalance in the Ang-2/Ang-1 ratio early after reperfusion. Representative cortical photomicrographs of kidney sections stained with Ang-1 (A) or Ang-2 (B) in a sham-operated rat and rats subjected to I/R and sacrificed at 72 hr or 9 weeks after reperfusion. Immunofluorescent double staining for Ang-1/NG2 (C), RECA-1/Ang-2 (D) and Ang-2/RECA-1 (E) of representative kidney sections in a sham-operated rat. Arrows indicate double staining in yellow (C,D) and apical expression of Ang-2 (E). Quantitative analysis of cortical protein expression of Ang-1 (F), Ang-2 (G), and Ang-2/Ang-1 ratio (H) at consecutive time points after reperfusion. Quantitative analysis of RNA expression of Ang-1 (I), Ang-2 (J) and Tie-2 (K) at consecutive time points after reperfusion. Data are shown as mean ± SEM (n= 5 rats per group). *P<0.05 compared to corresponding sham controls. #P<0.05 compared to 72 hr. Magnification of A-E, x400.

to 72 hr in the cortex and up to 9 weeks in both the outer and inner medulla (p< 0.05) (Fig. 5A, B). PDGFRβ expression showed normalization at the protein level in all regions of the kidney (p<0.05) at 9 weeks after renal I/R injury (Fig. 5A, B). To investigate the anatomical relation of ECs and pericytes double staining

with RECA-1 and the pericyte marker NG2 were performed, which revealed expression of both markers in the glomeruli and peritubular space (Fig. 5C).

Figure 5. Renal I/R induces proliferation of pericytes. Representative photo-micrographs of whole kidney sections stained for PDGFRβ (A) in a sham-operated rat and rats subjected to I/R and sacrificed at 72 hr or 9 weeks after reperfusion. Insert is showing peritubular and glomerular expression of PDGFRβ in sham-operated rats. Quantitative analysis of PDGFRβ protein expression (B) at consecutive time points after reperfusion. Fluorescent double staining for RECA-1 (red) and NG2 (green) of representative kidney sections (C) in a sham-operated rat and rat subjected to I/R and sacrificed at 9 weeks after reperfusion. Data are shown as mean ± SEM (n= 5 rats per group). *P<0.05 compared to corresponding sham controls. #P<0.05 compared to 72hr. Original magnification of A, x100; insert at 72hr and C, x200.

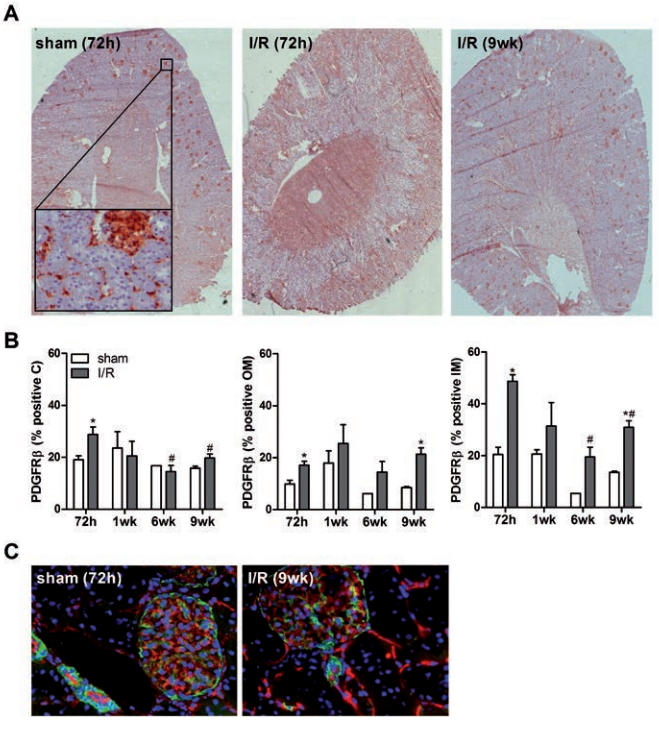

DISCUSSION

We performed a detailed kinetic analysis of angiopoietin and pericyte expression after renal I/R injury. We demonstrate that renal I/R induces a dysbalance in Ang-2/Ang-1 which is accompanied by a loss of ECs, proliferation of pericytes and development of fibrosis. At 9 weeks post I/R, we show reversal to baseline in Ang-2/Ang-1 balance, an increase in ECs and normalization of PDGFRβ expression in the cortex. Whereas renal function is fully restored at this time point, the renal tissue does still show signs of fibrosis.

It is postulated that loss of ECs is a central common pathway involved in organ failure that precedes and drives the profibrotic changes of the kidney parenchyma (2;3;24). Different reports using animal models have been

published which demonstrate chronic deleterious effects of ischemic injury on long-term renal function and microvascular structure (2;6;16;17;29;36). Basile et al have shown that renal I/R in a rat model results in permanent damage to peritubular capillaries with development of tubulointerstitial fibrosis and decline in long-term renal function (2). In the present study, we also observed loss of peritubular capillaries and development of tubulointerstitial fibrosis following renal I/R, which were more severe and extensive in the outer and inner medulla than the cortex. The observed fibrosis at early time points after renal I/R injury in our study coincided with the influx of inflammatory cells. At later time points, we observed a different pattern of fibrosis, which was more dense and unrelated to the areas of inflammation. This 'inflammatory fibrosis' observed at early times has been reported to be important for restoration of the original tissue morphology and function (13). It is, however, also suggested that if repair is not efficient at early times, fibrosis at the repair phase cannot be prevented (9). In our study, at 9 weeks after reperfusion, restoration and proliferation of ECs was found in the cortex, but not in the outer and inner medulla. This could be caused by the anatomical relationship of capillaries and tubules in the outer and inner medulla, with consequently a greater impact of hypoxia- and leucocyte-induced EC damage than in the cortical peritubular capillaries (5).

In contrast to the study of Basile et al, we found restoration and proliferation of ECs in the cortex in the repair phase (9 weeks after I/R). Possible explanations for this discrepancy between our study and the studies of Basile could be differences in clamping time (45 versus 60 minutes, respectively) and the removal of the healthy contralateral kidney in our study. In the study of Basile, additional experiments in which rats were subjected to 30 and 45 minutes of bilateral ischemia were performed, to assess whether the duration of ischemic injury affects damage to the renal microvasculature and function. Both renal function and capillary density were more disturbed in the 45 minutes group compared to the 30 minutes rats, which might implicate a "critical ischemia time" for endothelial repair (2).

The molecular mechanisms that lead to microvascular injury in organ failure are largely unknown. It has been suggested that several angioregulatory growth factors, including the angiopoeitins, play a central role in the loss of vascular integrity (18;36). In this regard, a study has shown that treatment with COMP-Ang-1 (soluble, stable and potent form of Ang-1) in a mice model of renal I/R resulted in protection against peritubular capillary damage, decrease in interstitial inflammatory cells and renal interstitial fibrosis (5). Other investigators have demonstrated stabilization of peritubular capillaries along with increased fibrosis and inflammation after adenoviral Ang-1 treatment in a mouse model of folic acid-induced nephrotoxicity (37). These studies suggest that differences

in efficacy of Ang-1 in the kidney may be due to variation in potency of Ang-1 and COMP-Ang-1 or difference in kidney disease models (5;12;37). Ang-2 acts as an antagonist of Ang-1 and increases vessel leakage, inflammation and destabilization by promoting pericyte loss, therefore loosening contacts between ECs and pericytes (18;36).

An interesting observation in this study is the relation in time between Ang-2/Ang-1 balance and microvascular integrity and pericytes in the cortex after I/R. Activation of ECs, reflected by increase in Ang-2 expression and consequently higher Ang-2/Ang-1 ratio, was accompanied by proliferation of pericytes, EC loss and development of fibrosis. This relation between EC loss and dysbalance in angiopoietins has also been demonstrated in a mouse model of anti-glomerular basement membrane glomerulonephritis, where glomerular capillary loss was associated with reduced Ang-1 and increased Ang-2 expression (38). In addition, in an animal model of diabetic retinopathy, Ang-1 was shown to have a profound effect in repairing integrity of the retinal EC permeability barrier (39). Moreover, injection of Ang-2 into the eyes of normal rats has been shown to induce a dose-dependent pericyte loss (28). These findings suggest an important role for the angiopoeitins in generating a proangiogenic environment that is necessary for capillary repair.

Several studies have pointed at the critical importance of the interaction between pericytes and ECs in maintenance of the capillary network (1;30). Surprisingly, hardly any data are available on the relation between pericytes and loss of ECs in renal I/R. Only one study has shown an association between damage to peritubular capillaries and decreased number of pericytes in cadaveric renal allografts after I/R (21). Peritubular capillary integrity was better preserved and pericytes were more pronounced in patients who had a better recovery of their graft function compared to patients with sustained postischemic acute kidney injury (21). However, this study investigated the expression of pericytes at only one time-point early after renal I/R and did not investigate the relation to angiopoietins and development of fibrosis in a time course.

To investigate the role of pericytes in renal I/R injury, we used PDGFRβ as pericyte marker. PDGFRβ is a single-spanning transmembrane glycoprotein that binds to its dimeric ligand PDGF and a crucial receptor for recruitment and survival of pericytes by paracrine secretion of PDGFB by ECs (4;23;33). PDGFRβ has been shown in studies of obstructive and post-ischemic kidney injury to be expressed by pericytes and fibroblasts (8;22;23). Compared with other pericyte markers, PDGFRβ continued to be expressed after proliferation of pericytes and after transformation into myofibroblasts upon injury. Recently, Duffield et al provided evidence for the contribution of pericytes to the development of renal fibrosis (11;18;23;30). Using a transgenic mouse model of unilateral ureter obstruction

(UUO), expressing green fluorescent protein in cells producing the collagen type I, they demonstrated that pericytes are the main source for interstitial myofibroblasts during renal fibrosis (23). The same investigators showed migration of perivascular stromal cells from capillaries into the renal interstitium, within 9 hr after induction of ureter obstruction. After loosening contact from the capillaries, pericytes became activated and proliferated into collagen producing myofibroblasts contributing to fibrosis (23). PDGFRβ signaling has been reported to play an important role in the development of fibrosis. Blockade of PDGFRβ attenuated recruitment of inflammatory cells, loss of ECs and fibrosis in mice subjected to renal I/R injury and UUO (22). Also in our study we demonstrated proliferation of pericytes and loss of ECs which was accompanied by development of fibrosis. The pericytes may have responded to injury by detaching from the capillaries and becoming pathologic matrix depositing cells, that contribute to the population of α-SMA–positive cells in the fibrotic interstitial space observed in this study (8;31). The process of pericyte detachment has been suggested to be reversible, which could explain the observed decrease in PDGFRβ expression and the restoration of ECs in the cortex (22). However, in both the inner and outer medulla an increase of PDGFRβ cells was observed up to 9 weeks after renal I/R. Interestingly, these areas had no increase in EC staining and demonstrated a more profound fibrosis reaction compared to the less damaged cortex area.

An important discussion point remains whether the decrease in RECA-1 in the cortex observed in our study is explained by EC loss or by interstitial edema and compression of peritubular capillaries. However, previous studies utilizing microfilm analyses and EC staining with CD31 confirmed the loss of ECs after I/R (2;3;17;19;32). Additional CD31 staining in this study revealed a similar pattern as observed with RECA-1. Although our study clearly suggests that angiopoietins are essential in renal microvascular remodeling in the cortex, we were not able to analyze the outer and inner medulla of Ang-2 staining. Ang-2 showed brush border and apical expression on tubules in the medulla, making it difficult to distinguish between interstitial and tubular presence of Ang-2. Therefore, we focused only on the cortex for angiopoietins staining. Furthermore, we observed a discrepancy in Ang-2 protein and mRNA expression, which could be explained by the use of whole kidney RNA extractions instead of a specific region as for immunohistochemistry or contribution of earlier produced Ang-2 by infiltrating cells, while lacking the detectable transcript (28). A therapeutic intervention would be required to prove a causal relationship between the functions of angiopoietins and pericytes and its role in EC stabilization and repair.

In conclusion, our study demonstrates that renal I/R induces a dysbalance in angiopoietins, accompanied by proliferation of pericytes and development of fibrosis. These findings support the hypothesis that angiopoietins and pericytes

play an important role in renal microvascular remodeling. Since angiopoietins and pericytes are considered as important hallmarks of microvascular integrity, strategies to counteract microvascular destabilization after I/R may well improve long term graft function.

GRANTS

This work was supported by a Veni grant from ZonMW (01086089) to M.E.J. Reinders and Dutch Kidney Foundation grants to P. van der Pol (NSN KSTP 11.005) and T.J. Rabelink (C 09.2329).

REFERENCES

1. Armulik A, Abramsson A, Betsholtz C. Endothelial/pericyte interactions. Circ Res 97: 512-523, 2005.
2. Basile DP, Donohoe D, Roethe K, Osborn JL. Renal ischemic injury results in permanent damage to peritubular capillaries and influences long-term function. Am J Physiol Renal Physiol 281: F887-F899, 2001.
3. Basile DP, Friedrich JL, Spahic J, Knipe N, Mang H, Leonard EC, et al. Impaired endothelial proliferation and mesenchymal transition contribute to vascular rarefaction following acute kidney injury. Am J Physiol Renal Physiol 300: F721-F733, 2011.
4. Bergers G, Song S. The role of pericytes in blood-vessel formation and maintenance. Neuro Oncol 7: 452-464, 2005.
5. Bonventre JV, Yang L. Cellular pathophysiology of ischemic acute kidney injury. J Clin Invest 121: 4210-4221, 2011.
6. Brodsky SV, Yamamoto T, Tada T, Kim B, Chen J, Kajiya F, et al. Endothelial dysfunction in ischemic acute renal failure: rescue by transplanted endothelial cells. Am J Physiol Renal Physiol 282: F1140-F1149, 2002.
7. Cai J, Kehoe O, Smith GM, Hykin P, Boulton ME. The angiopoietin/Tie-2 system regulates pericyte survival and recruitment in diabetic retinopathy. Invest Ophthalmol Vis Sci 49: 2163-2171, 2008.
8. Chen YT, Chang FC, Wu CF, Chou YH, Hsu HL, Chiang WC, et al. Platelet-derived growth factor receptor signaling activates pericyte-myofibroblast transition in obstructive and post-ischemic kidney fibrosis. Kidney Int 80: 1170-1181, 2011.
9. Contreras AG, Briscoe DM. Every allograft needs a silver lining. J Clin Invest 117: 3645-3648, 2007.
10. Duffield JS. The elusive source of myofibroblasts: problem solved? Nat Med 18: 1178-1180, 2012.
11. Duffield JS, Humphreys BD. Origin of new cells in the adult kidney: results from genetic labeling techniques. Kidney Int 79: 494-501, 2011.
12. Dulauroy S, Di Carlo SE, Langa F, Eberl G, Peduto L. Lineage tracing and genetic ablation of ADAM12(+) perivascular cells identify a major source of profibrotic cells during acute tissue injury. Nat Med 2012.
13. Farris AB, Colvin RB. Renal interstitial fibrosis: mechanisms and evaluation. Curr Opin Nephrol Hypertens 21: 289-300, 2012.
14. Feng Y, vom HF, Pfister F, Djokic S, Hoffmann S, Back W, et al. Impaired pericyte recruitment and abnormal retinal angiogenesis as a result of angiopoietin-2 overexpression. Thromb Haemost 97: 99-108, 2007.
15. Hammes HP, Lin J, Renner O, Shani M, Lundqvist A, Betsholtz C, et al. Pericytes and the pathogenesis of diabetic retinopathy. Diabetes 51: 3107-3112, 2002.
16. Hattori R, Ono Y, Kato M, Komatsu T, Matsukawa Y, Yamamoto T. Direct visualization of cortical peritubular capillary of transplanted human kidney with reperfusion injury using a magnifying endoscopy. Transplantation 79: 1190-1194, 2005.
17. Horbelt M, Lee SY, Mang HE, Knipe NL, Sado Y, Kribben A, et al. Acute and chronic microvascular alterations in a mouse model of ischemic acute kidney injury. Am J Physiol Renal Physiol 293: F688-F695, 2007.
18. Humphreys BD, Lin SL, Kobayashi A, Hudson TE, Nowlin BT, Bonventre JV, et al. Fate tracing reveals the pericyte and not epithelial origin of myofibroblasts in kidney fibrosis. Am J Pathol 176: 85-97, 2010.
19. Jung YJ, Kim DH, Lee AS, Lee S, Kang KP, Lee SY, et al. Peritubular capillary preservation with COMP-angiopoietin-1 decreases ischemia-reperfusion-induced acute kidney injury. Am J Physiol Renal Physiol 297: F952-F960, 2009.
20. Kida Y, Duffield JS. Pivotal role of pericytes in kidney fibrosis. Clin Exp Pharmacol Physiol 38: 417-423, 2011.
21. Kwon O, Hong SM, Sutton TA, Temm CJ. Preservation of peritubular capillary endothelial integrity and increasing pericytes may be critical to recovery from postischemic acute kidney injury. Am J Physiol Renal Physiol 295: F351-F359, 2008.
22. Lin SL, Chang FC, Schrimpf C, Chen YT, Wu CF, Wu VC, et al. Targeting endothelium-pericyte cross talk by inhibiting VEGF receptor signaling attenuates kidney microvascular rarefaction and fibrosis. Am J Pathol 178: 911-923, 2011.
23. Lin SL, Kisseleva T, Brenner DA, Duffield JS. Pericytes and perivascular fibroblasts are the primary source of collagen-producing cells in obstructive fibrosis of the kidney. Am J Pathol 173: 1617-1627, 2008.
24. Long DA, Norman JT, Fine LG. Restoring the renal microvasculature to treat chronic kidney disease. Nat Rev Nephrol 8: 244-250, 2012.
25. Molitoris BA, Sutton TA. Endothelial injury and dysfunction: role in the extension phase of acute renal failure. Kidney Int 66: 496-499, 2004.
26. Reinders ME, Rabelink TJ, Briscoe DM. Angiogenesis and endothelial cell repair in renal disease and allograft rejection. J Am Soc Nephrol 17: 932-942, 2006.
27. Roos-van Groningen MC, Scholten EM, Lelieveld PM, Rowshani AT, Baelde HJ, Bajema IM, et al. Molecular comparison of calcineurin inhibitor-induced fibrogenic responses in protocol renal transplant

biopsies. J Am Soc Nephrol 17: 881-888, 2006.
28. Sandhu R, Teichert-Kuliszewska K, Nag S, Proteau G, Robb MJ, Campbell AI, et al. Reciprocal regulation of angiopoietin-1 and angiopoietin-2 following myocardial infarction in the rat. Cardiovasc Res 64: 115-124, 2004.
29. Schmitz V, Schaser KD, Olschewski P, Neuhaus P, Puhl G. In vivo visualization of early microcirculatory changes following ischemia/reperfusion injury in human kidney transplantation. Eur Surg Res 40: 19-25, 2008.
30. Schrimpf C, Xin C, Campanholle G, Gill SE, Stallcup W, Lin SL, et al. Pericyte TIMP3 and ADAMTS1 Modulate Vascular Stability after Kidney Injury. J Am Soc Nephrol 23: 868-883, 2012.
31. Strutz F, Zeisberg M. Renal fibroblasts and myofibroblasts in chronic kidney disease. J Am Soc Nephrol 17: 2992-2998, 2006.
32. Sutton TA, Mang HE, Campos SB, Sandoval RM, Yoder MC, Molitoris BA. Injury of the renal microvascular endothelium alters barrier function after ischemia. Am J Physiol Renal Physiol 285: F191-F198, 2003.
33. Toffalini F, Hellberg C, Demoulin JB. Critical role of the platelet-derived growth factor receptor (PDGFR) beta transmembrane domain in the TEL-PDGFRbeta cytosolic oncoprotein. J Biol Chem 285: 12268-12278, 2010.
34. van der Pol P, Schlagwein N, van Gijlswijk DJ, Berger SP, Roos A, Bajema IM, et al. Mannan-binding lectin mediates renal ischemia/reperfusion injury independent of complement activation. Am J Transplant 12: 877-887, 2012.
35. Woolf AS, Gnudi L, Long DA. Roles of angiopoietins in kidney development and disease. J Am Soc Nephrol 20: 239-244, 2009.
36. Yamamoto T, Tada T, Brodsky SV, Tanaka H, Noiri E, Kajiya F, et al. Intravital videomicroscopy of peritubular capillaries in renal ischemia. Am J Physiol Renal Physiol 282: F1150-F1155, 2002.